

## Conformational study of ketoprofen by combined DFT calculations and Raman spectroscopy

M.L. Vueba<sup>a</sup>, M.E. Pina<sup>a</sup>, F. Veiga<sup>a</sup>, J.J. Sousa<sup>a</sup>, L.A.E. Batista de Carvalho<sup>b,\*</sup>

<sup>a</sup> Centro de Estudos Farmacêuticos (CEF), Laboratório de Galénica e Tecnologia Farmacêutica, Faculdade de Farmácia, Universidade de Coimbra, Rua do Norte, 3000-295 Coimbra, Portugal

<sup>b</sup> Unidade I&D “Química-Física Molecular”, Faculdade de Ciências e Tecnologia, Universidade de Coimbra, 3004-535 Coimbra, Portugal

Received 6 July 2005; accepted 24 September 2005

Available online 4 November 2005

### Abstract

A conformational study of ketoprofen was carried out by both density functional theory (DFT) calculations and Raman spectroscopy. Nine different geometries were found to correspond to energy minimum conformations but only one of them was experimentally detected in the condensed phase spectra.

Those rotations which interconvert the five most stable conformers were studied and the intramolecular interactions governing the corresponding conformational preferences were assessed.

A thorough vibrational analysis was performed, leading to the assignment of both the solid and liquid spectra. Evidence for formation of intermolecular hydrogen bonds between carboxylic groups of adjacent ketoprofen molecules, leading to dimeric entities, was obtained.

© 2005 Elsevier B.V. All rights reserved.

**Keywords:** Ketoprofen; DFT calculations; Raman spectroscopy; FTIR spectroscopy; Conformational analysis; Rotational isomerism

### 1. Introduction

The development process of solid pharmaceutical dosage forms should imply a previous thorough characterisation of the drugs, as most probably its solid-state structure has a relevant influence on both its stability and bioavailability (Byrn et al., 1994,1995). In fact, the conformational preferences of the drug may determine the chemical and/or physical mechanisms (i.e. intermolecular interactions), which control its release into the body from a particular delivery system.

Several methods can be applied in order to get structural information on a certain species as well as to understand interactions between this active agent and distinct compounds (excipients and/or carriers). Among them, Raman spectroscopy has been successfully used for the characterisation and quantification of various solid-state forms of drugs (Niemczyk et al., 1998; Marques et al., 2002; Szostak and Mazurek, 2002), including polymorphs (Deeley et al., 1991; Tudor et al., 1993; Forster et al., 1999), amorphous materials (Taylor and Zografi, 1997,1998)

and salts (Findlay and Bugay, 1998). Also, found in the literature are studies on the characterisation of drugs within different supports (Taylor and Langkilde, 2000), as polymeric matrices (Davies et al., 1990a,b; Watts et al., 1991; Breienbach et al., 1999; Kazarian and Martirosyan, 2002) or cyclodextrins (Choi et al., 2001).

Ketoprofen (Fig. 1A), chemically [2-(3-benzoylphenyl) propionic acid], a weak acid ( $pK_a = 4.6$ ), poorly water-soluble type drug (water solubility value  $\approx 0.13 \text{ mg/ml}^{-1}$  at  $25^\circ\text{C}$ ), is one type of “profen” class of non-steroid anti-inflammatory drug (NSAID). This drug contains a chiral center at the  $\alpha$ -carbon to the carboxyl function and therefore exists as  $R(-)$  and  $S(+)$  enantiomeric forms. According to Mullangi et al. (2003), its anti-inflammatory activity, as determined by in vivo cyclo-oxygenase inhibition, resides almost exclusively with the  $S$ -enantiomer. Ketoprofen has been shown to act as an analgesic, antipyretic and anti-inflammatory effects, and used for the treatment of rheumatoid arthritis, osteoarthritis and ankylosis spondylitis (Cathcart et al., 1973; Fossgreen, 1976; Fossgreen et al., 1976; Julou et al., 1976), and also for non-rheumatoid diseases (Avouac and Teule, 1988). Its mechanism of action is mainly based on inhibitory effects on prostaglandin and leukotrien synthesis (Vargaftig and Dao, 1971), as well as antibradykinin effects and lysosomal

\* Corresponding author. Tel.: +351 239854462; fax: +351 239826541.  
E-mail address: [labc@ci.uc.pt](mailto:labc@ci.uc.pt) (L.A.E.B. de Carvalho).

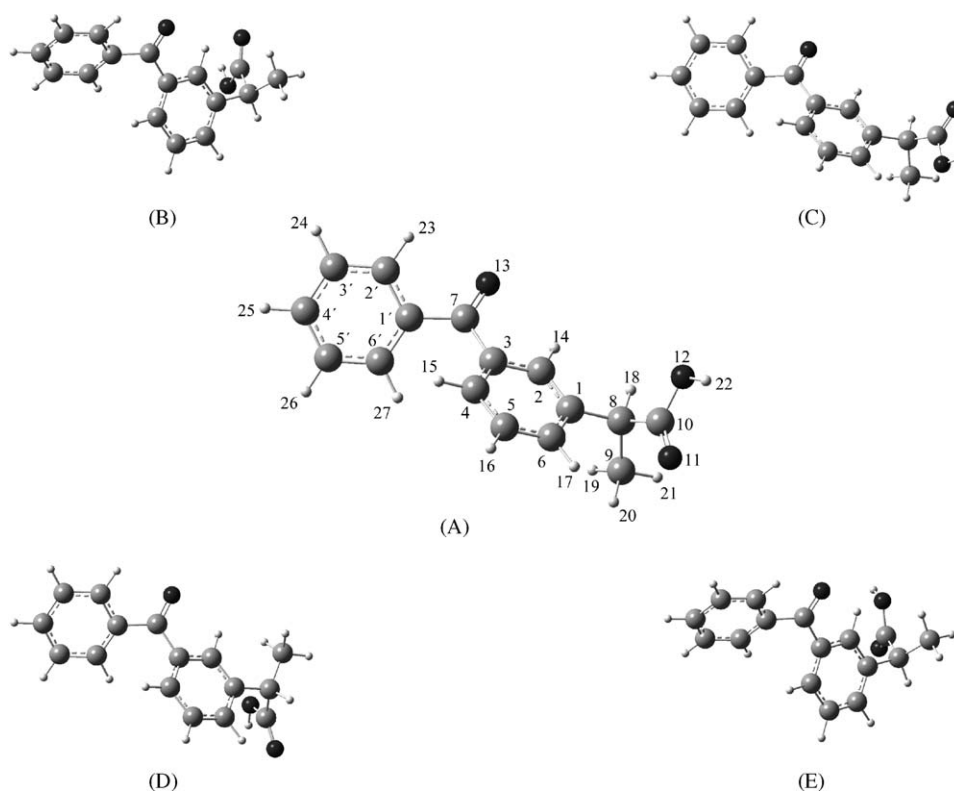


Fig. 1. (A–E) Schematic representation of the five most stable conformers of ketoprofen molecule.

membrane stabilising activity (Stiegler et al., 1995). Ketoprofen's half-life in blood plasma was found to be between 2 and 3 h (Martindale, 1996). This short half-life, coupled to the low single administration dosage necessary, renders ketoprofen a very good candidate for the formulation of controlled release dosage forms (Caruso et al., 1982; Houghton et al., 1984a,b; Marcolongo et al., 1984; Morley et al., 1984; Giunchedi et al., 1991; Le Liboux et al., 1994; Habib and Meuse, 1995; Khan et al., 1996; Parejo et al., 1998; Vergote et al., 2001; Roda et al., 2002; Palmieri et al., 2002; Vueba et al., 2004). However, the exact nature of the mechanisms underlying drug controlled release processes is still unknown.

Raman spectroscopy, long established as a non-invasive method particularly adequate to study both intra- and intermolecular interactions, allows a comparative investigation of drug performance, in the solid state, either when mixed with the required excipients in the formulation of the matrix tablets or in other pharmaceutical dosage forms (Breienbach et al., 1999; Scranton et al., 2000; Vankeirsbilck et al., 2002; Vergote et al., 2002, 2004; De Beer et al., 2004). Moreover, Raman spectroscopy can be applied without any particular sample preparation, thus avoiding mechanical influences, which may alter the physicochemical properties of the formulation. In order to perform this kind of study, the conformational preferences of the ketoprofen molecule must be previously determined and assignment of its Raman features should be carried out. This could be achieved with the help of MO calculations.

The possibility of preparing ketoprofen hydrophilic matrix tablets using cellulosic polymers and different required excipi-

ents, has lately become more and more important, as extended-release (either constant or pulsed) dosage forms of the drug may often be beneficial. Thus, the knowledge of intermolecular interactions between ketoprofen and these polymers/excipients, which regulates the drug release processes within the body, is of the utmost importance. This may be accomplished through Raman spectroscopy, once the conformational behaviour of the pure drug in the solid state is known. The present study aims at achieving this goal, which will hopefully allow to carry out future studies on ketoprofen tablets (composed of distinct drug/polymer/excipient mixtures).

In this work, a conformational study on ketoprofen was undertaken by Raman spectroscopy combined to DFT calculations. The FTIR spectrum of ketoprofen in a KBr disk was also analysed, in order to explore the well known complementary between these two optical vibrational spectroscopy techniques.

## 2. Materials and methods

### 2.1. Chemicals

Ketoprofen, batch no. 043K0684, was purchased from Sigma–Aldrich Chemie, Germany.

### 2.2. Raman spectroscopy

The Raman spectra were obtained on a triple monochromator Jobin-Yvon T64000 Raman system (focal distance

0.640 m, aperture  $f/7.5$ ) equipped with holographic gratings of 1800 grooves  $\text{mm}^{-1}$ . The premonochromator stage was used in the subtractive mode. The detection system was liquid nitrogen cooled non-intensified  $578 \times 385$  pixel (1/2 in.) charge coupled device (CCD) chip. A Coherent (model Innova 300-05)  $\text{Ar}^+$  laser was used as light source, the output of which at 514.5 nm was adjusted to provide 35 mW at the sample position. A  $90^\circ$  geometry, between the incident radiation and the collecting system, was employed. The entrance slit was set to 200  $\mu\text{m}$  and the slit between the premonochromator and the spectrograph was opened to 12 mm. An integration time of 3 s and 10–15 scans were used in all experiments.

Samples were sealed in Kimax glass capillary tubes of 0.8 mm inner diameter. Under the above-mentioned conditions, the error in wavenumbers was estimated to be within  $1 \text{ cm}^{-1}$ .

A home-made Harney–Miller type assembly (Miller and Harney, 1970) was used for recording the spectrum of liquid ketoprofen which required a temperature of ca. 370 K.

### 2.3. FTIR spectroscopy

Infrared spectra of ketoprofen in KBr disks (ca. 5%, w/w) were recorded at room temperature on a Nicolet Model 740 FTIR spectrometer, in the range  $400\text{--}4000 \text{ cm}^{-1}$ , using a global source, a Ge/KBr beamsplitter, a DTGS detector. The spectra were collected in 32 scans to a 16,384 data points file (resolution ca.  $2 \text{ cm}^{-1}$ ) and subject to a Happ–Genzel apodisation. The errors in wavenumbers were estimated to less than  $1 \text{ cm}^{-1}$ .

### 2.4. DFT calculations

The molecular orbital calculations were carried out with the GAUSSIAN 98W program (Frisch et al., 1998), within the density functional theory (DFT) approach, using the B3LYP method, which includes a mixture of Hartree–Fock (HF) and DFT exchange terms. The gradient-corrected correlation functional was used (Lee et al., 1988; Miehlich et al., 1989), parameterised after Becke (1988, 1993), along with the double-zeta split valence basis set 6-31G\* (Hariharan and Pople, 1973).

Molecular geometries were fully optimised by the Berny algorithm, using redundant internal coordinates (Peng et al., 1996): the bond lengths to within ca. 0.1 pm and the bond angles to within ca.  $0.1^\circ$ . The final root-mean-square (rms) gradients

were always less than  $3 \times 10^{-4}$  Hartree bohr $^{-1}$  or Hartree rad $^{-1}$ . In order to study the barriers to internal rotation, the geometries were optimised for different fixed internal rotation angles.

The quantitative potential energy deconvolution was based on least-squares fitted Fourier type functions of a torsional angle,

$$V = V_0 + \sum_{n=1}^3 \frac{1}{2} V_n [1 - \cos(n\tau)] + \sum_{n=1,2,4} V'_n \sin(n\tau)$$

where  $\tau$  is the  $\text{HC}_8\text{C}_1\text{C}_6$  dihedral angle (Fig. 1) and  $V$  are functional values that correspond to potential energy differences relative to a reference value ( $V_0$  is the energy corresponding to a  $\text{HC}_8\text{C}_1\text{C}_6$  angle of  $0^\circ$ ).

## 3. Results and discussion

### 3.1. Conformational analysis

Ketoprofen molecule can adopt different conformations, mainly by varying the dihedral angles around the  $\text{C}_1\text{--C}_8$ ,  $\text{C}_8\text{--C}_{10}$  and  $\text{C}_{10}\text{--O}_{12}$  bonds (Fig. 1). Conformational energy minima not separated by more than  $7 \text{ kJ mol}^{-1}$  from the most stable conformer are shown in Fig. 1. Table 1 comprises the conformational energy differences, dipole moments and rotational constants of all the conformers found. The *s-trans* arrangement ( $\text{O}=\text{C}\text{--O}\text{--H}$  angle ca.  $180^\circ$ , not shown in Fig. 1), whenever present, was found to be significantly less stable (by about  $18 \text{ kJ mol}^{-1}$ ) than their *s-cis* counterpart ( $\text{O}=\text{C}\text{--O}\text{--H}$  angle ca.  $0^\circ$ , Fig. 1), and is referred to along the text using primes (e.g.  $A'$  and  $A$ , respectively, for conformer A) (Fig. 2).

The results now obtained were to be expected in view of the conclusions from previous conformational studies on propionic and 2-methylpropionic acids (Siam et al., 1984; Batista de Carvalho et al., 1990; Teixeira-Dias et al., 1991). In fact, in these kinds of molecules, the preferred conformations around the  $\text{C}_\alpha\text{--C}$  bond are the ones displaying  $\alpha$ -substituents with either *syn* or *skew* orientations relative to the  $\text{C}=\text{O}$  bond ( $\text{CCC}=\text{O}$  equals  $0^\circ$  or  $\pm 120^\circ$ , respectively).

Table 2 comprises the B3LYP/6-31G\* optimised geometry calculated for the most stable conformation (results for the other conformers and parameters involving hydrogen atoms are available from the authors upon request), as well as the X-ray experimental geometry determined by Briard and Rossi (1990).

Table 1  
Conformational energies, dipole moments ( $\mu$ ) and rotational constants calculated for the ketoprofen conformers

Conformation	$\text{HC}_8\text{C}=\text{O}; \text{HC}_8\text{C}_1\text{C}_6$ ( $^\circ$ )	$\Delta E$ ( $\text{kJ mol}^{-1}$ )	$\mu^a$ (D)	A; B; C (GHz)
A	−157.9; −169.1	0.00	2.12	1.095; 0.157; 0.149
B	−150.1; 7.4	2.15	4.09	0.818; 0.178; 0.170
C	15.0; −173.7	6.12	4.41	1.096; 0.157; 0.148
D	20.2; −44.1	6.42	2.21	0.909; 0.169; 0.161
E	17.4; 2.1	5.51	2.20	0.832; 0.177; 0.169
A'	−109.5; −176.0	18.8	5.79	1.113; 0.158; 0.150
B'	−100.7; 1.6	22.2	6.54	0.835; 0.175; 0.169
C'	25.1; −147.9	34.3	5.96	1.126; 0.154; 0.148
E'	28.4; 5.3	31.9	4.29	0.821; 0.178; 0.169

<sup>a</sup> 1 D =  $1/3 \times 10^{-2}$  C m.

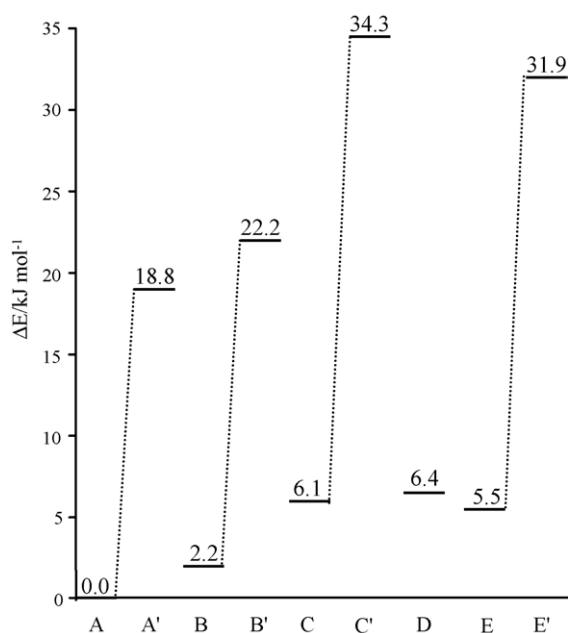


Fig. 2. Schematic representation of the conformational energies calculated for ketoprofen conformers.

The quantum mechanical results now obtained are in quite good agreement with the experimental ones.

It is worthwhile to note that the two aromatic rings of the ketoprofen molecule are not coplanar (Fig. 1). In fact, the planes containing the C<sub>3</sub>–C<sub>4</sub> and C<sub>1'</sub>–C<sub>6'</sub> bonds, for instance, were found, for all conformers, to define a dihedral angle of ca. 50° in good accordance with X-ray experimental value of 53° (Briard and Rossi, 1990).

Rotational isomerism in this kind of compounds – containing both aromatic rings, carbonyl and carboxylic groups – is influenced by different factors, from steric, dipolar, mesomeric and hyperconjugative effects, to hydrogen bonding interactions. Moreover, the relative importance of intramolecular versus intermolecular interactions (e.g. dimer formation) has often proved, in several systems, to be determinant of their conformational preferences, either as pure compounds or in solution.

Once the *s-cis* conformers are significantly more stable than *s-trans* ones (Fig. 2), the rotational isomerism around the C<sub>1</sub>–C<sub>8</sub> bond for a HOC=O dihedral ca. 0° (*s-cis*) was studied. Two particular cases were considered: HC<sub>8</sub>C=O ca. –155° or 15°, corresponding to energy minima around the C<sub>8</sub>–C<sub>10</sub> internal rotation. The C<sub>1</sub>–C<sub>8</sub> rotation converts conformers A to B (Fig. 3a), as well as C to D and E (Fig. 4a), for HC<sub>8</sub>C=O ca. –155° and 15°, respectively.

The energy difference between B and the more stable A conformer is 2.15 kJ mol<sup>-1</sup>, the corresponding internal rotation barrier (A → B) being 12.3 kJ mol<sup>-1</sup> (Fig. 3a). Considering the values of the Fourier components of the potential energy dependence on this rotation (Fig. 3b and c), it can be concluded that the largely dominant contribution is represented by a cosine term in V<sub>2</sub> (11.0 kJ mol<sup>-1</sup>), thus favouring those conformations where steric hindrance is minimised, mainly by displaying the most voluminous groups – both methyl and carboxyl – away from the

Table 2

Calculated (B3LYP/6-31G\*) and experimental (X-ray; Briard and Rossi, 1990) geometrical parameters for the most stable conformer (A) of ketoprofen

Coordinate <sup>a</sup>	Experimental	Calculated
<b>Bond length (pm)</b>		
C <sub>2</sub> –C <sub>1</sub>	136.7	139.4
C <sub>6</sub> –C <sub>1</sub>	138.5	140.4
C <sub>8</sub> –C <sub>1</sub>	153.2	152.8
C <sub>3</sub> –C <sub>2</sub>	139.3	140.4
C <sub>4</sub> –C <sub>3</sub>	139.5	140.2
C <sub>7</sub> –C <sub>3</sub>	148.8	150.2
C <sub>5</sub> –C <sub>4</sub>	138.1	139.5
C <sub>6</sub> –C <sub>5</sub>	139.2	139.4
O <sub>13</sub> –C <sub>7</sub>	121.8	122.6
C <sub>1'</sub> –C <sub>7</sub>	148.7	150.1
C <sub>9</sub> –C <sub>8</sub>	151.8	154.0
C <sub>10</sub> –C <sub>8</sub>	151.5	152.3
O <sub>11</sub> –C <sub>10</sub>	124.8	121.3
O <sub>12</sub> –C <sub>10</sub>	125.4	135.3
C <sub>2'</sub> –C <sub>1'</sub>	138.8	140.4
C <sub>6'</sub> –C <sub>1'</sub>	139.3	140.4
C <sub>3'</sub> –C <sub>2'</sub>	137.8	139.1
C <sub>4'</sub> –C <sub>3'</sub>	136.7	139.8
C <sub>5'</sub> –C <sub>4'</sub>	137.4	139.6
C <sub>6'</sub> –C <sub>5'</sub>	138.2	139.5
<b>Bond angle (°)</b>		
C <sub>6</sub> –C <sub>1</sub> –C <sub>2</sub>	118.6	118.8
C <sub>8</sub> –C <sub>1</sub> –C <sub>2</sub>	119.8	120.2
C <sub>8</sub> –C <sub>1</sub> –C <sub>6</sub>	121.5	121.1
C <sub>3</sub> –C <sub>2</sub> –C <sub>1</sub>	121.4	121.3
C <sub>4</sub> –C <sub>3</sub> –C <sub>2</sub>	119.8	119.1
C <sub>7</sub> –C <sub>3</sub> –C <sub>2</sub>	118.6	117.5
C <sub>7</sub> –C <sub>3</sub> –C <sub>4</sub>	121.5	123.2
C <sub>5</sub> –C <sub>4</sub> –C <sub>3</sub>	119.1	119.9
C <sub>6</sub> –C <sub>5</sub> –C <sub>4</sub>	120.1	120.4
C <sub>5</sub> –C <sub>6</sub> –C <sub>1</sub>	121.1	120.4
O <sub>13</sub> –C <sub>7</sub> –C <sub>3</sub>	119.6	119.6
C <sub>1'</sub> –C <sub>7</sub> –C <sub>3</sub>	121.4	120.7
C <sub>1'</sub> –C <sub>7</sub> –O <sub>13</sub>	119.0	119.7
C <sub>9</sub> –C <sub>8</sub> –C <sub>1</sub>	112.4	111.9
C <sub>10</sub> –C <sub>8</sub> –C <sub>1</sub>	110.3	109.7
C <sub>10</sub> –C <sub>8</sub> –C <sub>9</sub>	110.0	110.2
O <sub>11</sub> –C <sub>10</sub> –C <sub>8</sub>	119.1	125.4
O <sub>12</sub> –C <sub>10</sub> –C <sub>8</sub>	117.6	120.0
O <sub>12</sub> –C <sub>10</sub> –O <sub>11</sub>	123.3	122.6
C <sub>2'</sub> –C <sub>1'</sub> –C <sub>7</sub>	118.9	117.7
C <sub>6'</sub> –C <sub>1'</sub> –C <sub>7</sub>	122.5	123.1
C <sub>6'</sub> –C <sub>1'</sub> –C <sub>2'</sub>	118.5	119.1
C <sub>3'</sub> –C <sub>2'</sub> –C <sub>1'</sub>	120.4	120.5
C <sub>4'</sub> –C <sub>3'</sub> –C <sub>2'</sub>	120.6	120.0
C <sub>5'</sub> –C <sub>4'</sub> –C <sub>3'</sub>	119.9	119.9
C <sub>6'</sub> –C <sub>5'</sub> –C <sub>4'</sub>	120.2	120.1
C <sub>5'</sub> –C <sub>6'</sub> –C <sub>1'</sub>	120.3	120.3
<b>Torsional angle (°)</b>		
C <sub>2</sub> –C <sub>1</sub> –C <sub>8</sub> –C <sub>10</sub>	116.0	129.0
C <sub>6</sub> –C <sub>1</sub> –C <sub>8</sub> –C <sub>10</sub>	–67.6	–52.4
C <sub>1</sub> –C <sub>8</sub> –C <sub>10</sub> –O <sub>11</sub>	72.2	85.1
C <sub>1</sub> –C <sub>8</sub> –C <sub>10</sub> –O <sub>12</sub>	–107.3	–93.6
C <sub>2</sub> –C <sub>3</sub> –C <sub>7</sub> –C <sub>1'</sub>	159.3	154.5
C <sub>4</sub> –C <sub>3</sub> –C <sub>7</sub> –C <sub>1'</sub>	–25.3	–29.5
C <sub>3</sub> –C <sub>7</sub> –C <sub>1'</sub> –C <sub>2'</sub>	147.5	153.8
C <sub>3</sub> –C <sub>7</sub> –C <sub>1'</sub> –C <sub>6'</sub>	–36.0	–30.1

<sup>a</sup> See Fig. 1 for atom numbering.

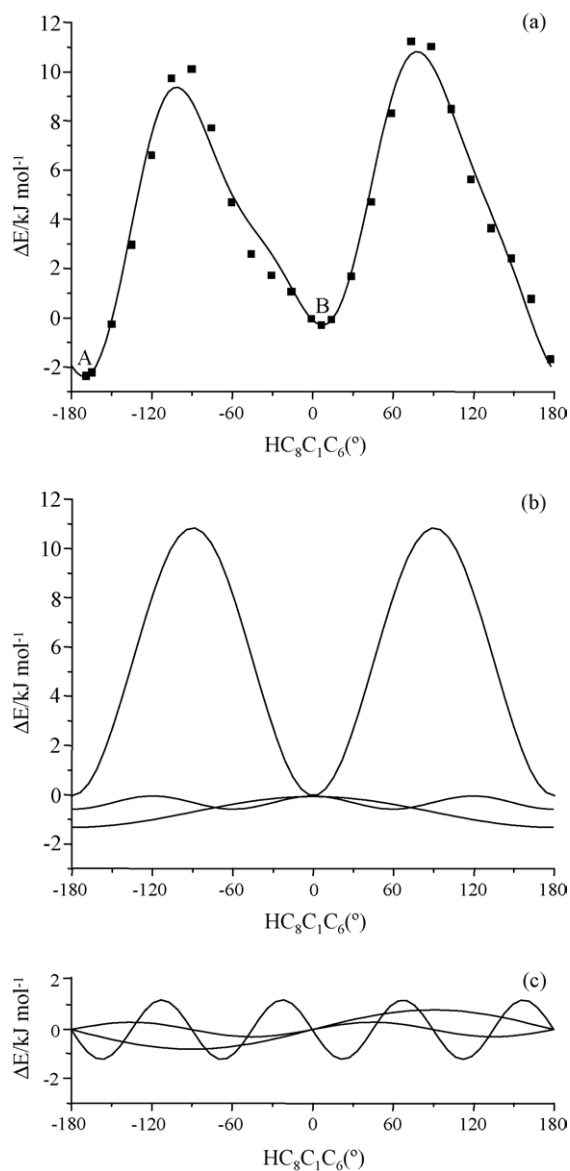


Fig. 3. Optimised (B3LYP/6-31G\*) conformational energy profile for the internal rotation around the C<sub>1</sub>–C<sub>8</sub> bond of ketoprofen for HC<sub>8</sub>C=O ca. –155° (a) and its Fourier deconvolution (b and c).

closest phenyl, which corresponds to the geometries where each of the former are positioned above and below the ring (dihedral HC<sub>8</sub>C<sub>1</sub>C<sub>6</sub> being either 0° or 180°).

The  $V_1$  term ( $-1.41 \text{ kJ mol}^{-1}$ ) favours those conformations having a HC<sub>8</sub>C<sub>1</sub>C<sub>6</sub> dihedral close to 180°, which reflects the stronger attractive interaction between the C<sub>10</sub>=O<sub>11</sub> carbonyl group and the H<sub>17</sub> atom in conformer A – giving rise to a six-membered intramolecular ring – as compared to the interaction between this carbonyl group and the H<sub>14</sub> hydrogen in geometry B. Moreover, the greater stabilisation of the A conformer relative to B may be explained in terms of the balance between the following factors (Fig. 5): the stabilising interaction due to the presence, in both geometries, of a bifurcated H<sub>23</sub> ↔ O<sub>13</sub> ↔ H<sub>14</sub> acceptor; the bifurcated O<sub>13</sub> ↔ H<sub>14</sub> ↔ O<sub>11</sub> donor interaction which occurs in B; and the O<sub>11</sub> ↔ H<sub>17</sub> hydrogen bond found in A. In fact, the sharing of H<sub>14</sub> between two adjacent H-type

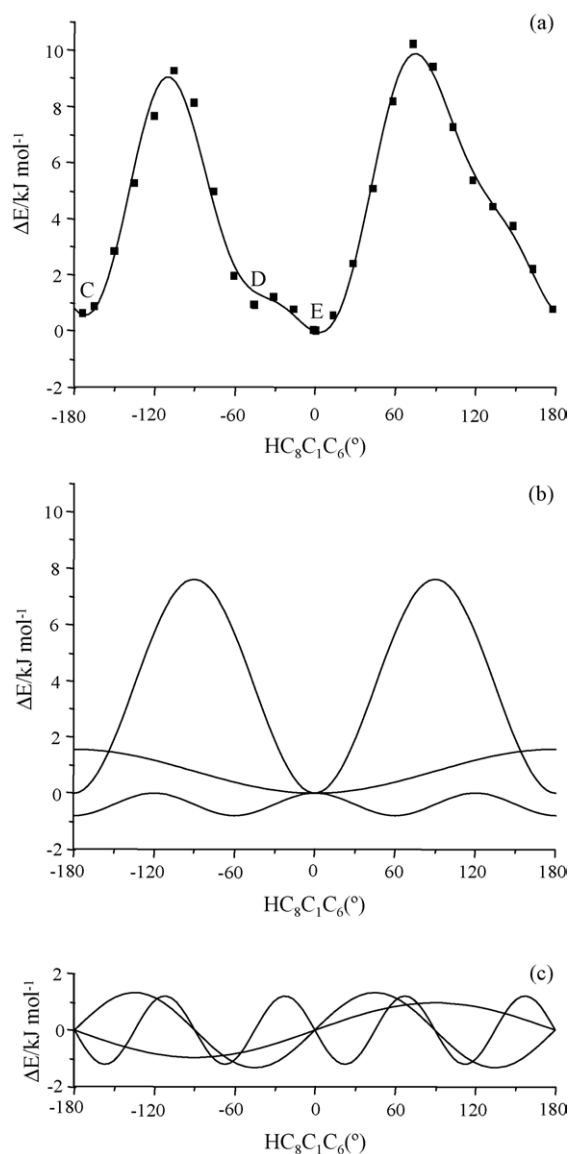


Fig. 4. Optimised (B3LYP/6-31G\*) conformational energy profile for the internal rotation around the C<sub>1</sub>–C<sub>8</sub> bond of ketoprofen for HC<sub>8</sub>C=O ca. 15° (a) and its Fourier deconvolution (b and c).

bonds is, in this particular molecule, an energetically unfavouring factor, as it is responsible for a significant weakening of the H<sub>14</sub> ↔ O<sub>11</sub> interaction ( $d_{\text{H}_{14}\text{O}_{11}}$  equal to 281 pm, in B, versus  $d_{\text{H}_{17}\text{O}_{11}}$  equal to 261 pm, in A).

The  $V_3$  term ( $-0.60 \text{ kJ mol}^{-1}$ ), in turn, reflects the steric hindrance between the H<sub>17</sub> atom and any one of the C<sub>8</sub> substituents (either H, COOH or CH<sub>3</sub>). Thus, energy maxima occur for a

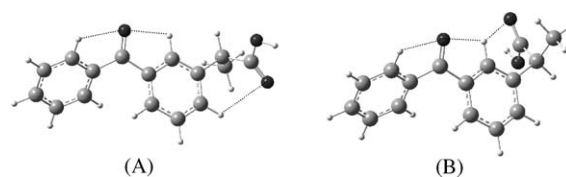


Fig. 5. Schematic representation of the intramolecular interactions found in the A and B ketoprofen conformers.

$\text{HC}_8\text{C}_1\text{C}_6$  dihedral equal to  $0^\circ$ ,  $120^\circ$  and  $-120^\circ$ , while minima are detected for  $60^\circ$ ,  $180^\circ$  and  $-60^\circ$  (Fig. 3b).

As to the sine terms, the most important one was found to be  $V'_4$  [ $-1.22 \text{ kJ mol}^{-1}$ , Fig. 3c]. This contribution can be explained in the light of electrostatic factors occurring within the molecule. In fact, it displays maxima for those conformations where repulsive interactions arise, between the positively charged  $\text{H}_{19}$  and  $\text{H}_{20}$  methyl hydrogens and the aromatic  $\text{H}_{14}$  or  $\text{H}_{17}$  atoms. On the other hand,  $V'_4$  presents energy minima whenever the methyl group is positioned such as to minimise this kind of destabilising interactions: either above or below the ring plane, in a perpendicular position; or, alternatively, with  $\text{C}_9$  and  $\text{H}_{21}$  in the ring plane, and both  $\text{H}_{19}$  and  $\text{H}_{20}$  positioned symmetrically relative to  $\text{H}_{14}$  or  $\text{H}_{17}$  atoms.

On the other hand, the three conformers displaying a  $\text{HC}_8\text{C}=\text{O}$  dihedral of ca.  $15^\circ$  are about  $3\text{--}6 \text{ kJ mol}^{-1}$  higher than A and B (Table 1; Fig. 2). The following potential energy differences were calculated:  $-0.30 \text{ kJ mol}^{-1}$  for  $\Delta E(\text{C}\text{--}\text{D})$ ,  $0.91 \text{ kJ mol}^{-1}$  for  $\Delta E(\text{D}\text{--}\text{E})$  and  $0.61 \text{ kJ mol}^{-1}$  for  $\Delta E(\text{C}\text{--}\text{E})$ , while the barrier of internal rotation converting conformer C into D/E is  $8.3 \text{ kJ mol}^{-1}$  (Fig. 4a). Interesting enough is the detection of an unexpected minimum – species D – for  $\text{HC}_8\text{C}_1\text{C}_6$  equal to  $-44.1^\circ$  (Fig. 4), which is confirmed beyond doubt by the absence of negative calculated vibrational frequencies for this geometry. This low energy conformer arises from a  $\text{H}_{17} \leftrightarrow \text{O}_{11}$  hydrogen bond type interaction ( $d_{\text{H}_{17}\text{O}_{11}}$  equal to 281 pm). However, the rotation barrier corresponding to the D to E interconversion process is surprisingly small – ca.  $0.3 \text{ kJ mol}^{-1}$  – corresponding, in fact, to a free rotation process for temperatures above 36 K. Thus, despite its low conformational energy, the population of conformer D should not be significant, once the energy of the first vibrational level (calculated value:  $0.23 \text{ kJ mol}^{-1}$ ) and this rotational barrier are of the same order of magnitude. Actually, the torsion associated to the  $\text{HC}_8\text{C}_1\text{C}_6$  dihedral, probably displaying a rather large amplitude, is proposed to be the process responsible for the  $\text{D} \leftrightarrow \text{E}$  interconversion.

Moreover, conformer D' is not detected, once the stabilisation due to the occurrence of a  $\text{H}_{17} \leftrightarrow \text{O}_{11}$  intermolecular interaction (previously described) is overruled by the geometrical rearrangement associated to the presence of the hydroxyl  $\text{H}_{22}$  atom near the  $\text{CH}_3$  group (which, in turn, is in close proximity to the  $\text{H}_{14}$  hydrogen; Fig. 1).

When comparing the graphic representations and their Fourier components, for both rotational processes studied (Figs. 3 and 4), it can be concluded that there is an obvious similarity between them. Thus, independently of their magnitude, the  $V_2$  [ $7.65 \text{ kJ mol}^{-1}$ , Fig. 4b],  $V_3$  [ $-0.79 \text{ kJ mol}^{-1}$ , Fig. 4b] and  $V'_4$  [ $-1.20 \text{ kJ mol}^{-1}$ , Fig. 4c] terms could be interpreted in the light of the same type of interactions as the ones described above. On the other hand, the  $V_1$  term [ $1.58 \text{ kJ mol}^{-1}$ , Fig. 4b] exhibits an inverse behaviour relative to  $\text{HC}_8\text{C}_1\text{C}_6$  dihedral angle: conformations with this dihedral close to  $0^\circ$  are the preferred ones. The greater stabilisation of the E conformer relative to C could be almost completely explained by the examination of the magnitude of electrostatic interactions present in both. Actually, in the E conformer the  $\text{H}_{14} \leftrightarrow \text{O}_{12}$  stabilising interaction (Mulliken charges: 0.174 and  $-0.562$ ,

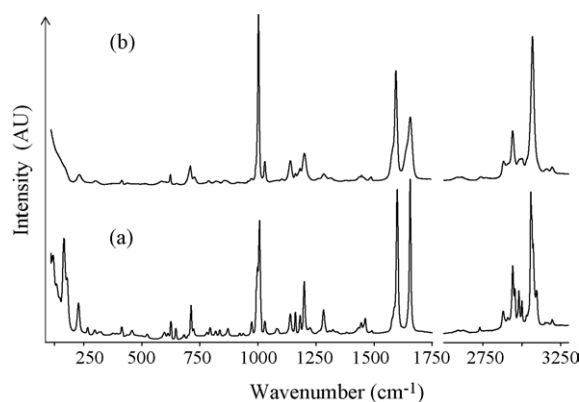


Fig. 6. Raman spectra ( $100\text{--}1750$  and  $2500\text{--}3300 \text{ cm}^{-1}$ ) of ketoprofen in the: solid (a) and liquid (b) phases.

respectively;  $d = 264.0 \text{ pm}$ ) is stronger than the  $\text{H}_{17} \leftrightarrow \text{O}_{12}$  one present in the C conformer (Mulliken charges: 0.152 and  $-0.564$ , respectively;  $d = 251.5 \text{ pm}$ ). Comparing repulsive relations, in turn, the  $\text{H}_{17} \leftrightarrow \text{H}_{18}$  destabilising interaction in the E conformer (Mulliken charges: 0.138 and 0.165, respectively;  $d = 228.0 \text{ pm}$ ) is weaker than the  $\text{H}_{14} \leftrightarrow \text{H}_{18}$  one present in the C conformer (Mulliken charges: 0.165 and 0.177, respectively;  $d = 230.0 \text{ pm}$ ).

### 3.2. Vibrational analysis

Fig. 6 comprises the Raman spectra for both the solid and liquid ketoprofen, in the  $100\text{--}1750$  and  $2500\text{--}3300 \text{ cm}^{-1}$  regions. Fig. 7 contains the FTIR spectrum for solid ketoprofen, in the  $400\text{--}1800$  and  $2300\text{--}3500 \text{ cm}^{-1}$  intervals. Experimental Raman and FTIR wavenumbers are presented in Table 3, along with the DFT calculated values for the two most stable conformers, A and B (Fig. 1). The agreement between the experimental and calculated wavenumbers, after scaling according to Scott and Radom (1996) in order to correct for the unharmonicity of the normal modes of vibration, was found to be rather good. In fact, as the calculated energy difference between B and the most stable A conformer is only  $2.15 \text{ kJ mol}^{-1}$ , either of these conformers may have significant populations at room temperature. However, the calculated values for the low frequency region (below  $600 \text{ cm}^{-1}$ ), which is the most conformationally sensitive one, are remarkably consistent with the sole presence of conformer A, both for liquid and solid ketoprofen.

Table 3 also contains the complete assignment of ketoprofen observed bands to the normal modes of vibration. It is

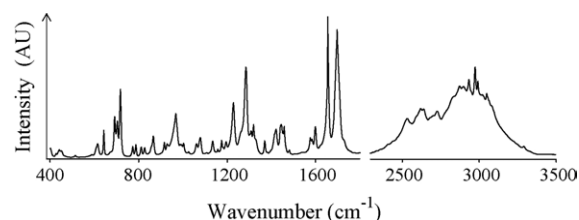


Fig. 7. FTIR spectrum ( $400\text{--}1800$  and  $2300\text{--}3500 \text{ cm}^{-1}$ ) of solid ketoprofen in a KBr disk.

Table 3  
 Experimental (Raman and FTIR) and DFT MO-calculated harmonic wavenumbers ( $\text{cm}^{-1}$ ) and intensities for ketoprofen

Raman		FTIR	Calculated <sup>a</sup>		Approximate descriptions <sup>b</sup>
Liquid	Solid		Conformer A	Conformer B	
	110			96 (6; 0)	$\text{C}^7\text{--}\phi\text{--}\text{C}^8$ wagging (10b)
	124		117 (7; 1)		$\text{C}^7\text{--}\phi\text{--}\text{C}^8$ wagging (10b)
	138		136 (1; 1)	140 (2; 2)	$\text{C}^7\text{=O}^{13}$ out-of-plane bending
	157		148 (4; 2)		$\phi'\text{--}\text{C}^7$ wagging (10b)
	170		184 (1; 0)		$\text{CH}_3\text{--}\text{C--}\phi$ deformation; $\text{C}^7\text{--}\phi\text{--}\text{C}^8$ bending (10a)
223	220		220 (6; 1)	201 (5; 0)	$\phi'\text{--}\text{C}^7$ wagging (10b); $\text{C}^7\text{--}\phi\text{--}\text{C}^8$ wagging (10b)
			229 (0; 0)	230 (1; 0)	$\text{C}^7\text{--}\phi\text{--}\text{C}^8$ bending (10a); $\phi'\text{--}\text{C}^7\text{--}\phi$ deformation
				236 (3; 1)	$\text{CH}_3\text{--}\text{C}$ torsion
260	259		253 (1; 2)	254 (0; 4)	$\text{C}^7\text{--}\phi\text{--}\text{C}^8$ bending (10a); $\text{CH}_3\text{--}\text{C}$ torsion
294	290		296 (4; 1)	300 (2; 0)	$\text{CH}_3\text{--}\text{C--}\text{C(=O)}$ deformation
	310		–	–	$\text{CH}_3\text{--}\text{C--}\phi$ deformation; ( $\text{O}^{13}\text{=C}^7$ )– $\phi'$ torsion
	317		–	–	Overtone ( $2 \times 157 \text{ cm}^{-1}$ )
	370		369 (1; 1)	357 (2; 1)	Combination mode ( $157 + 170 \text{ cm}^{-1}$ )
	385		385 (1; 7)	384 (1; 8)	$\text{C}^7\text{--}\phi\text{--}\text{C}^8$ bending G (15); $\text{C--}\text{C--}\text{OH}$ deformation
408	408		421 (2; 0)	419 (2; 0)	$\text{C}^7\text{=O}^{13}$ in-plane bend; $\phi$ , $\phi'$ out-of-plane bend (16b)
432	430	427	432 (3; 7)	436 (1; 4)	$\phi'$ out-of-plane bending (16a)
		441	441 (1; 0)	446 (1; 5)	$\text{C--}\text{C--}\text{OH}$ deformation
446	453	450	456 (1; 3)	454 (1; 4)	$\phi$ out-of-plane bending (16b)
508	518	514	513 (2; 3)	515 (3; 1)	$\phi'$ out-of-plane bending (16b)
582	593	588	570 (4; 15)	552 (3; 10)	$\text{C--}\text{O--}\text{H}$ bending; $\phi$ out-of-plane bending (16a)
	608	608	588 (6; 37)	592 (6; 22)	$\text{C--}\text{O--}\text{H}$ bending
			608 (5; 0)	607 (4; 12)	$\phi$ (16a), $\phi'$ (16b) out-of-plane bend; $\text{C--}\text{O--}\text{H}$ bend
620	621	614			$\phi'$ in-plane bending (6b)
			615 (5; 64)	609 (5; 46)	$\text{C--}\text{O--}\text{H}$ out-of-plane bending
			630 (3; 15)	636 (4; 20)	$\text{C--}\text{O--}\text{H}$ out-of-plane bend; $\phi$ , $\phi'$ in-plane bend (6a)
647	642	642			
			642 (4; 73)	634 (3; 90)	$\text{C--}\text{O--}\text{H}$ bending; $\phi$ (6b), $\phi'$ (6a) in-plane bending
	677	671	677 (1; 10)	675 (2; 8)	$\phi$ , $\phi'$ out-of-plane bending (4)
	696	691	688 (3; 9)	685 (11; 14)	$\phi$ out-of-plane bend (4); $\phi'$ CH out-of-plane bend (11)
706	708	703	692 (9; 22)	689 (4; 21)	$\phi'$ CH out-of-plane bend (11); $\phi$ out-of-plane bend (4)
724	718	717	708 (4; 54)	707 (4; 52)	$\phi$ , $\phi'$ CH out-of-plane bending (11)
			750 (1; 12)	745 (1; 14)	$\text{C--}\text{O--}\text{H}$ out-of-plane bending
	776	773			
			773 (3; 11)	770 (2; 4)	$\phi$ , $\phi'$ CH out-of-plane wagging
787	790	787	792 (4; 12)		$\text{CH}_3$ rocking
				803 (3; 39)	$\text{CH}_3$ rocking; $\phi$ CH out-of-plane wagging
~821	814	811	808 (4; 11)		$\phi$ CH out-of-plane wagging
	832	827	837 (6; 3)	836 (5; 3)	$\phi'$ CH out-of-plane bending (10a)
	856	857			
~858	867	866	830 (6; 47)	826 (5; 26)	$\text{C--}\text{O--}\text{H}$ in-plane bending; $\text{CH}_3$ rocking
914	918	916	916 (1; 2)	915 (2; 3)	$\phi'$ (17b), $\phi$ (17a) CH out-of-plane bending
931	934	929	922 (1; 0)	917 (2; 5)	$\phi$ (17a), $\phi'$ (17b) CH out-of-plane bending
959			946 (1; 1)	943 (3; 5)	$\phi'$ (17a) CH out-of-plane bending
972	970	968	951 (7; 32)	945 (3; 24)	$\text{CH}_3$ rock; $\phi$ ring deformation (7b); $\phi$ CH bend (17b)
		987	968 (1; 1)	967 (1; 1)	$\phi'$ CH out-of-plane bending (5)
	996	993	975 (27; 3)	978 (20; 2)	$\phi$ ring deformation (12); $\text{CH}_3$ rocking
1003					
	1005	1003	979 (35; 0)	980 (58; 1)	$\phi'$ ring deformation (12)
1030	1028	1026	1018 (18; 1)	1019 (14; 1)	$\phi'$ CH in-plane bending (18a)
1065	1066	1061	1065 (1; 15)	1070 (2; 15)	$\text{CH}_3$ rocking
1082	1081	1078	1059 (4; 47)	1050 (2; 34)	$\text{CH}_3$ rock; $\text{C--}\text{CH}_3$ stretching; $\text{C--}\text{O--}\text{H}$ in-plane bend
1104	1108	1106	1090 (6; 5)	1088 (10; 24)	$\phi$ CH in-plane bending (18a)
1141	1138	1135	1119 (18; 13)	1116 (16; 13)	$\phi\text{--}\text{C--}\phi'$ symmetric stretch
1163	1160	1158	1149 (7; 1)	1148 (8; 0)	$\phi'$ CH in-plane bending (9b)
		1175	1163 (5; 38)	1162 (4; 21)	$\phi$ (9b), $\phi'$ (9a) CH in-plane bending
1182	1180	1182	1167 (6; 14)	1166 (7; 22)	$\phi$ (9b), $\phi'$ (9a) CH in-plane bending
1202	1198	1196	1178 (68; 49)	1178 (56; 34)	$\phi$ , $\phi'$ ring deform (13), $\text{C}_1'\text{--}\text{C}_7$ , $\text{C}_1\text{--}\text{C}_8$ stretching
	1223	1228	1137 (3; 225)	1136 (4; 210)	$\text{C--}\text{O--}\text{H}$ in-plane bend; $\text{C--}\text{O}$ stretching
1262	1262	1260	1245 (7; 22)	1238 (13; 139)	$\phi$ CH in-plane bending (3); $\text{C--}\text{O--}\text{H}$ in-plane bending
1286	1281	1285	1252 (21; 301)	1255 (13; 165)	$\phi$ , $\phi'$ ring deform (13), $\text{C}_1'\text{--}\text{C}_7\text{--}\text{C}_3$ antisymmetric stretch

Table 3 (Continued)

Raman		FTIR	Calculated <sup>a</sup>		Approximate descriptions <sup>b</sup>
Liquid	Solid		Conformer A	Conformer B	
	1306	1309	1305 (2; 3) 1315 (2; 2)	1310 (2; 14) 1315 (3; 2)	$\phi$ CH in-plane bending (3); C <sub>8</sub> –H bending $\phi'$ C–C stretching (14)
1316	1321	1320	1317 (5; 4)	1318 (3; 12)	
	1340	~1330			
	1370	1370	1364 (2; 45)	1357 (3; 58)	C <sub>10</sub> –C <sub>8</sub> –H deformation
1381	1382	1382	1381 (3; 11)	1386 (3; 6)	CH <sub>3</sub> symmetric deformation
	1421	1421	1424 (10; 35)	1424 (6; 17)	$\phi$ C–C stretching (19a); C <sub>1</sub> –C <sub>8</sub> –H deformation
1440	1434	1444	1435 (4; 17)	1435 (4; 16)	$\phi'$ C–C stretching (19b)
1450	1445		1463 (14; 4)	1462 (16; 4)	CH <sub>3</sub> antisymmetric deformation
~1460	1462	1457	1468 (18; 11)	1469 (17; 8)	CH <sub>3</sub> antisymmetric deformation
~1485	1484	1481	1472 (4; 4)	1472 (2; 7)	$\phi$ C–C stretching (19b); CH <sub>3</sub> antisymmetric deform
1491	1491		1480 (5; 1) 1573 (7; 6)	1480 (5; 1) 1573 (6; 6)	$\phi'$ C–C stretching (19a) $\phi'$ C–C stretching (8b)
	~1579	1576			
			1574 (34; 9)	1575 (27; 8)	$\phi$ C–C stretching (8a)
~1584	~1588	1584	1590 (125; 17)	1590 (117; 21)	$\phi$ C–C stretching (8b)
1600	1601	1599	1594 (115; 15)	1594 (117; 16)	$\phi'$ C–C stretching (8a)
1662	1657	1655	1671 (142; 141)	1674 (133; 122)	C <sub>7</sub> =O <sub>13</sub> stretching
	~1705	1697	1763 (5; 229)	1770 (5; 225)	C <sub>10</sub> =O <sub>11</sub> stretching (H-bonded)
		2539	–	–	Combination mode
2590	2590	~2595	–	–	Combination mode
2618	2625	2626	–	–	Combination mode
		2645	–	–	Combination mode
2737	2731	2734	–	–	Combination mode
2884	2881	2879	–	–	Combination mode
2913	2912	2905	–	–	Combination mode
2942	2942	2939			
	2956	~2954	2945 (141; 24)	2948 (138; 24)	CH <sub>3</sub> symmetric stretching
2987	2982	2979	2972 (45; 6)	2961 (67; 11)	C <sub>8</sub> –H <sub>18</sub> stretching
3003	3001	2997	3011 (110; 29)	3013 (112; 28)	CH <sub>3</sub> antisymmetric stretching
~3030	3030	3026	3030 (31; 13)	3034 (28; 13)	CH <sub>3</sub> antisymmetric stretching
	3058	3054	3063 (51; 0)	3062 (51; 0)	$\phi'$ C–H stretching
	3065	~3061	3069 (63; 7)	3061 (69; 6)	$\phi$ C–H stretching
3069	3073	~3069	3073 (142; 13)	3073 (138; 11)	$\phi'$ C–H stretching
		~3088	3083 (133; 35)	3083 (160; 31)	$\phi'$ C–H stretching
			3085 (31; 4)	3094 (29; 1)	C <sub>2</sub> –H <sub>14</sub> stretching
			3097 (172; 11)	3096 (179; 11)	$\phi'$ , $\phi$ C–H stretching
	3096				
			3100 (157; 7)	3100 (152; 7)	$\phi'$ C–H stretching
	3151				Overtone/combination mode
3160					
	3166				Overtone/combination mode
3195	3195				Overtone/combination mode
		3295	3535 (183; 52)	3537 (150; 48)	OH stretching (H-bonded)

<sup>a</sup> At the B3LYP/6-31G\* level of calculation; wavenumbers above 600 cm<sup>-1</sup> scaled by a factor of 0.9614 (Scott and Radom, 1996); in parentheses: Raman scattering activities in Å u<sup>-1</sup> and infrared intensities in km mol<sup>-1</sup>.

<sup>b</sup> The commonly used Wilson notation for descriptions of benzene derivatives normal vibrations (Wilson, 1934; Varsányi, 1974) is presented inside parentheses.

worthwhile to mention that most of the observed frequencies can be considered as group frequencies, i.e. highly localised to a particular group within the ketoprofen molecule. From these assignments, it may be concluded that the experimental vibrational spectra confidently reflect the presence of specific intermolecular interactions. In particular, bands at 1705 and 3295 cm<sup>-1</sup>, assigned to C<sub>10</sub>=O<sub>11</sub> and O–H stretching vibrations, respectively, display a downward shift relative to the calculated values for the isolated molecule (Table 3), due to intermolecular

hydrogen bond type interactions. These close-contacts, which occur through the carboxylic groups of adjacent molecules, are responsible for the presence of ketoprofen dimeric entities in condensed phases. These conclusions are corroborated by the upward shifts detected for the C–O–H deformation modes (Table 3).

It should also be mentioned that ketoprofen dimer formation does not seem to involve a noticeable conformational rearrangement, each monomer retaining its minimum energy geometry.

#### 4. Conclusions

The MO calculations yield nine different energy minimum conformations. In general, the two aromatic rings of the ketoprofen molecule are not coplanar and the *s-trans* arrangement of the carboxylic group, whenever present, is found to be significantly less stable (by about 18 kJ mol<sup>-1</sup>) than the *s-cis* counterpart. This energy difference rules out the occurrence of a significant population of *s-trans* conformers, at room temperature.

Intra- and intermolecular CH...O weak hydrogen bonds have been extensively studied (Desiraju and Steiner, 1999 and references therein) and are often determinant of the conformational characteristics of the systems, both in the solid and in solution. In the ketoprofen molecule presently investigated these kind of interactions are, as discussed above, of the utmost importance. In fact, they are responsible for the stabilisation of two particular conformers (A and B) relative to all other calculated minimum energy geometries (Table 1).

Despite the small energy difference (2.15 kJ mol<sup>-1</sup>) between these two most stable conformers, the optical vibrational spectroscopy results allow to conclude that only the lowest energy geometry is present both in the liquid and solid phases of ketoprofen. Furthermore, evidence of intermolecular hydrogen bonds between carboxylic groups of adjacent ketoprofen molecules, leading to dimers, is also obtained.

The disruption of the dimeric species present in condensed phases could be one of the key factor for the understanding of the kinetic behaviour and drug release properties of ketoprofen containing controlled release systems.

#### Acknowledgments

M.L. Vueba acknowledges Ph.D. fellowship from Gabinete de Relações Internacionais da Ciência e do Ensino Superior (GRICES) and Fundação para Ciência e Tecnologia (FCT) for the financial support (Portugal). The authors thank Prof. M.P.M. Marques (Química-Física Molecular, University of Coimbra) for the helpful discussions.

#### References

- Avouac, B., Teule, M., 1988. Ketoprofen: the European experience. *J. Clin. Pharmacol.* 28, S2–S7.
- Batista de Carvalho, L.A.E., Teixeira-Dias, J.J.C., Fausto, R., 1990. The CH<sub>3</sub>CH<sub>2</sub> internal rotation in thiopropionic acid as studied by ab initio SCF-MO method. *J. Mol. Struct. (Theochem.)* 208, 109–121.
- Becke, A., 1988. Density-functional exchange-energy approximation with correct asymptotic behavior. *Phys. Rev. A* 38, 3098.
- Becke, A., 1993. Density-functional thermochemistry. III. The role of exact exchange. *J. Chem. Phys.* 98, 5648.
- Breienbach, J., Schrof, W., Neumann, J., 1999. Confocal Raman spectroscopy: analytical approach to solid dispersions and mapping of drugs. *Pharm. Res.* 16, 1109–1113.
- Briard, P., Rossi, J.C., 1990. Kétoprofène. *Acta Cryst.* C46, 1036–1038.
- Byrn, S.R., Pfeiffer, R.R., Stephenson, G., Grant, D.J.W., Gleason, W.B., 1994. Solid-state pharmaceutical chemistry. *Chem. Mater.* 6, 1148–1158.
- Byrn, S.R., Pfeiffer, R.R., Ganey, M., Hoiberg, C., Pochikian, G., 1995. Pharmaceutical solids: a strategic approach to regulatory considerations. *Pharm. Res.* 12, 945–954.
- Caruso, I., Frigerio, E., Fumagalli, M., Liverta, C., Moro, L., Tamassia, V., 1982. Bioavailability study on a new slow-release formulation of ketoprofen. *J. Int. Med. Res.* 10, 229–233.
- Cathcart, B.J., Vince, J.D., Gordon, A.J., Bell, M., Chalmers, I.M., 1973. Studies on 2-(3-benzoylphenyl) propionic acid ('Orudis'). *Ann. Rheum. Dis.* 32, 62–65.
- Choi, S.-H., Kim, S.-Y., Ryoo, J.J., Park, J.Y., Lee, K.-P., 2001. FT-Raman and FT-IR spectra of the non-steroidal antiinflammatory drug ketoprofen included in cyclodextrins. *Anal. Sci.* 17, i785–i788.
- Davies, M.C., Binns, J.S., Melia, C.D., Hendra, P.J., Bourgeois, D., Church, S.P., Stephenson, P.J., 1990a. FT Raman spectroscopy of drugs in polymers. *Int. J. Pharm.* 66, 223–232.
- Davies, M.C., Binns, J.S., Melia, C.D., Bourgeois, D., 1990b. Fourier transform raman spectroscopy of polymeric biomaterials and drug delivery systems. *Spectrochim. Acta* 46A, 277–283.
- De Beer, T.R.M., Vergote, G.J., Baeyens, W.R.G., Remon, J.P., Vervaet, C., Verpoort, F., 2004. Development and validation of a direct, non-destructive quantitative method for medroxyprogesterone acetate in a pharmaceutical suspension using FT-Raman spectroscopy. *Eur. J. Pharm. Sci.* 23, 355–362.
- Deeley, C.M., Spragg, R.A., Threlfall, T.L., 1991. A comparison of Fourier transform infrared and near-infrared Fourier transform raman spectroscopy for quantitative measurements: an application in polymorphism. *Spectrochim. Acta* 47A, 1217–1223.
- Desiraju, G.R., Steiner, T., 1999. *The Weak Hydrogen Bond in Structural Chemistry and Biology*. IUCr Monographs on Crystallography, vol. 9. Oxford University Press.
- Findlay, W.P., Bugay, D.E., 1998. Utilization of Fourier transform-Raman spectroscopy for the study of pharmaceutical crystal forms. *J. Pharm. Biomed. Anal.* 16, 921–930.
- Forster, A., Gordon, K., Schmierer, D., Soper, N., Wu, V., Rades, T., 1999. Characterisation of two polymorphic forms of Ranitine-HCl. *Internet J. Vibrational Spectrosc.* 2 (2), 12.
- Fossgreen, J., 1976. Ketoprofen-survey of current publications. *Scand. J. Rheumatol.*, 7–32.
- Fossgreen, J., Kirchheiner, B., Petersen, F.O., Tophøj, E., Zachariae, E., 1976. Clinical evaluation of ketoprofen (19.583 R.P.) in rheumatoid arthritis-double-blind cross-over comparison with indomethacin. *Scand. J. Rheumatol.*, 93–98.
- Frisch, M.J., et al., 1998. Gaussian 98W, Revision A.9. Gaussian, Inc., Pittsburgh, PA.
- Giunchedi, P., Maggi, L., Conte, U., Caramella, C., 1991. Ketoprofen pulsatile absorption from 'multiple unit' hydrophilic matrices. *Int. J. Pharm.* 77, 177–181.
- Habib, M.J., Meuse, R., 1995. Development of controlled release formulations of ketoprofen for oral use. *Drug Dev. Ind. Pharm.* 21, 1463–1472.
- Hariharan, P.C., Pople, J.A., 1973. The influence of polarization functions on molecular orbital hydrogenation energies. *Theor. Chim. Acta* 28, 213.
- Houghton, G.W., Dennis, M.J., Rigler, E.D., Parsons, R.L., 1984a. Comparative pharmacokinetics of ketoprofen derived from single oral doses of ketoprofen capsules or a novel sustained-release pellet formulation. *Biopharm. Drug Dispos.* 5, 203–209.
- Houghton, G.W., Dennis, M.J., Templeton, R., Calvert, R.M., Cresswell, D.G., 1984b. A pharmacokinetic study of repeated doses of a new controlled release of ketoprofen. *Int. Clin. Pharm. Ther.* 23, 131–133.
- Julou, L., Guyonnet, J.C., Ducrot, R., Fournel, J., Pasquet, J., 1976. Ketoprofen (19.583 R.P.) (2-(3-benzoylphenyl)-propionic acid). Main pharmacological properties: outline of toxicological and pharmacokinetic data. *Scand. J. Rheumatol.*, 33–44.
- Kazarian, S.G., Martirosyan, G.G., 2002. Spectroscopy of polymer/drug formulations processed with supercritical fluids: in situ ATR-IR and Raman study of impregnation of ibuprofen into PVP. *Int. J. Pharm.* 232, 81–90.
- Khan, M.A., Dib, J., Reedy, I.K., 1996. Statistical optimization of ketoprofen-eudragit S100 coprecipitates to obtain controlled release tablets. *Drug Dev. Ind. Pharm.* 22, 135–141.
- Lee, C., Yang, W., Parr, R.G., 1988. Development of the Colle-Salvetti correlation-energy formulation into a functional of the electron density. *Phys. Rev. B* 37, 785.

- Le Liboux, A., Teule, M., Frydman, A., Osterhuis, B., Jonkman, J.H.G., 1994. Effect of diet on the single- and multiple-dose pharmacokinetics of sustained-release ketoprofen. *Eur. J. Clin. Pharmacol.* 47, 361–366.
- Marcolongo, R., Rubegni, M., Provvedi, D., Giordano, N., Frati, E., Bruni, G., 1984. A double-blind, interpatient comparison of plain and slow-release ketoprofen in osteoarthritis. *Int. J. Clin. Pharm. Ther.* 22, 377–381.
- Marques, M.P.M., Oliveira, P.J., Moreno, A.J.M., Batista de Carvalho, L.A.E., 2002. Study of carvedilol by combined Raman spectroscopy and ab initio MO calculations. *J. Raman Spectrosc.* 33, 778–783.
- Martindale, 1996. *The Extra Pharmacopeia*. The Pharmaceutical Press, London.
- Miehlich, B., Savin, A., Stoll, H., Preuss, H., 1989. Results obtained with the correlation energy density functionals of Becke and Lee, Yang and Parr. *Chem. Phys. Lett.* 157, 200.
- Miller, F.A., Harney, B.M., 1970. Variable temperature sample holder for Raman spectroscopy. *Appl. Spectrosc.* 24, 291–292.
- Morley, K.D., Bernstein, R.M., Hughes, G.R.V., Black, C.M., Rajapakse, C.A.N., Wilson, L., 1984. A comparative trial of a controlled-release formulation of ketoprofen ('oruvail') and a conventional capsule formulation of ketoprofen ('orudis') in patients with osteoarthritis of the hip. *Curr. Med. Res. Opin.* 9, 28–34.
- Mullangi, R., Yao, M., Srinivas, N.R., 2003. Resolution of enantiomers of ketoprofen by HPLC a review. *Biomed. Chromatogr.* 17, 423–434.
- Niemczyk, T.M., Delgado-Lopez, M., Allen, J.T., Arneberg, D.L., 1998. Quantitative assay of bucindolol in gel capsules using infrared and Raman spectroscopy. *Appl. Spectrosc.* 4, 513–518.
- Palmieri, G.F., Bonacucina, G., Di Martino, P., Martilli, S., 2002. Microencapsulation of semisolid ketoprofen/polymer microspheres. *Int. J. Pharm.* 242, 175–178.
- Parejo, C., Gallardo, A., San Roman, J., 1998. Controlled release of NSAIDs bound to polyacrylic carrier systems. *J. Mater. Sci. Mater. Med.* 9, 803–809.
- Peng, C., Ayala, P.Y., Schlegel, H.B., Frisch, M.J., 1996. Using redundant internal coordinates to optimize equilibrium geometries and transition states. *J. Comput. Chem.* 17, 49.
- Roda, A., Sabatini, L., Mirasoli, M., Baraldini, M., Roda, E., 2002. Bioavailability of a new ketoprofen formulation for once-daily oral administration. *Int. J. Pharm.* 241, 165–172.
- Scott, A.P., Radom, L., 1996. Harmonic vibrational frequencies: an evaluation of Hartree–Fock, Møller–Plesset, quadratic configuration interaction, density functional theory, and semiempirical scale factors. *J. Phys. Chem.* 100, 16502–16513.
- Scranton, A.B., Drescher, B., Nelson, E.W., Jacobs, J.L., 2000. Use of infrared and Raman spectroscopy for characterization of controlled release systems. In: Wise, D.L. (Ed.), *Handbook of Pharmaceutical Controlled Release Technology*. Marcel Dekker, Inc., New York, pp. 131–153 (Chapter 7).
- Siam, K., Klimkowski, V.J., Ewbank, J.D., Schäfer, L., Van Alsenoy, C., 1984. Ab initio studies of structural features not easily amenable to experiment. 38. Structural and conformational investigations of propanoic, 2-methylpropanoic, and butanoic acid. *J. Comput. Chem.* 5, 451–456.
- Stiegler, S., Birkel, M., Jost, V., Lange, R., Lückner, P.W., Wetzelsberger, N., 1995. Pharmacokinetics and relative bioavailability after single dose administration of 25 mg ketoprofen solution as compared to tablets. *Methods Find. Exp. Clin. Pharmacol.* 17, 129–134.
- Szostak, R., Mazurek, S., 2002. Quantitative determination of acetylsalicylic acid and acetaminophen in tablets by FT-Raman spectroscopy. *Analyst* 127, 144–148.
- Taylor, L.S., Zografi, G., 1997. Spectroscopic characterization of interactions between PVP and indomethacin in amorphous molecular dispersions. *Pharm. Res.* 14, 1691–1698.
- Taylor, L.S., Zografi, G., 1998. The quantitative analysis of crystallinity using FT-Raman spectroscopy. *Pharm. Res.* 15, 755–761.
- Taylor, L.S., Langkilde, F.W., 2000. Evaluation of solid-state forms present in tablets by Raman spectroscopy. *J. Pharm. Sci.* 89, 1342–1353.
- Teixeira-Dias, J.J.C., Fausto, R., Batista de Carvalho, L.A.E., 1991. The C<sub>α</sub>–C internal rotation in α-alkyl substituted carbonyls and thiocarbonyls: CH(CH<sub>3</sub>)<sub>2</sub>C(=X)YH (X, Y=O or S). *J. Comput. Chem.* 12, 1047–1057.
- Tudor, A.M., Church, S.J., Hendra, P.J., Davies, M.C., Melia, C.D., 1993. The qualitative and quantitative analysis of chlorpropamide polymorphic mixtures by near-infrared Fourier transform raman spectroscopy. *Pharm. Res.* 10, 1772–1776.
- Vargafitig, B.B., Dao, N., 1971. Relative of vasoactive substances from guinea-pig lungs by slow-reacting substance C and arachidonic acid. Its blockade by nonsteroid anti-inflammatory agents. *Pharmacology* 6, 99–108.
- Vankeirsbilck, T., Vercauteren, A., Baeyens, W., Van, D.W., 2002. Applications of Raman spectroscopy in pharmaceutical analysis. *Trends Anal. Chem.* 12, 869–877.
- Varsányi, G., 1974. *Assignments for Vibrational Spectra of Seven Hundred Benzene Derivatives*. Akadémiai Kiadó, Budapest/Adam Hilger Ltd., London.
- Vergote, G.J., Vervaet, C., Van Driessche, I., Hoste, S., De Smedt, S., Demeester, J., Jain, R.A., Ruddy, S., Remon, J.P., 2001. An oral controlled release matrix pellet formulation containing nanocrystalline ketoprofen. *Int. J. Pharm.* 219, 81–87.
- Vergote, G.J., Vervaet, C., Remon, J.P., Haemers, T., Verpoort, F., 2002. Near-infrared FT-Raman spectroscopy as a rapid analytical tool for the determination of diltiazem hydrochloride in tablets. *Eur. J. Pharm. Sci.* 16, 63–67.
- Vergote, G.J., De Beer, T.R.M., Vervaet, C., Remon, J.P., Baeyens, W.R.G., Dierix, N., Verpoort, F., 2004. In-line monitoring of a pharmaceutical blending process using FT-Raman spectroscopy. *Eur. J. Pharm. Sci.* 21, 479–485.
- Vueba, M.L., Batista de Carvalho, L.A.E., Veiga, F., Sousa, J.J., Pina, M.E., 2004. Influence of cellulose ether polymers on ketoprofen release from hydrophilic matrix tablets. *Eur. J. Pharm. Biopharm.* 58, 51–59.
- Watts, P.J., Tudor, A., Church, S.J., Hendra, P.J., Turner, P., Melia, C.D., Davies, M.C., 1991. Fourier transform Raman spectroscopy for the qualitative and quantitative characterization of sulfasalazine-containing polymeric microspheres. *Pharm. Res.* 8, 1323–1328.
- Wilson Jr., E.B., 1934. The normal modes and frequencies of vibration of regular plane hexagon model of benzene molecule. *Phys. Rev.* 45, 706–714.